

QIRL: Boosting Visual Question Answering via Optimized Question-Image Relation Learning

Quanxing Xu¹, Ling Zhou¹, Xian Zhong², *Senior Member, IEEE*, Feifei Zhang³,
Rubing Huang⁴, *Senior Member, IEEE*, and Chia-Wen Lin⁵, *Fellow, IEEE*

Abstract—Existing debiasing approaches in Visual Question Answering (VQA) primarily focus on enhancing visual learning, integrating auxiliary models, or employing data augmentation strategies. However, these methods exhibit two major drawbacks. First, current debiasing techniques fail to capture the superior relation between images and texts because prevalent learning frameworks do not enable models to extract deeper correlations from highly contrasting samples. Second, they do not assess the relevance between the input question and image during inference, as no prior work has examined the degree of input relevance in debiasing studies. Motivated by these limitations, we propose a novel framework, **Optimized Question-Image Relation Learning (QIRL)**, which employs a generation-based self-supervised learning strategy. Specifically, two modules are introduced to address the aforementioned issues. The **Negative Image Generation (NIG)** module automatically produces highly irrelevant question-image pairs during training to enhance correlation learning, while the **Irrelevant Sample Identification (ISI)** module improves model robustness by detecting and filtering irrelevant inputs, thereby reducing prediction errors. Furthermore, to validate our concept of reducing output errors through filtering unrelated question-image inputs, we propose a specialized metric to evaluate the performance of the ISI module. Notably, our approach is model-agnostic and can be integrated with various VQA models. Extensive experiments on VQA-CPv2 and VQA-V2 demonstrate the effectiveness and generalization ability of our method. Among data augmentation strategies, our approach achieves state-of-the-art results.

Index Terms—Multi-modal, visual question answering, debiasing studies, question-image relation learning, self-supervised learning.

Manuscript received April 4, 2025. This work is supported in part by the Science and Technology Development Fund of Macau, Macau SAR, under Grant 0035/2023/ITP1 and 0021/2023/RIA1, the National Natural Science Foundation of China under Grant 62271361, and the Hubei Provincial Key Research and Development Program under Grant 2024BAB039. (Corresponding authors: Ling Zhou and Xian Zhong)

Quanxing Xu and Ling Zhou are with the School of Computer Science and Engineering, Macau University of Science and Technology, Taipa, Macau 999078, China (email: 3230002299@student.must.edu.mo; lzhou@must.edu.mo).

Xian Zhong is with the Hubei Key Laboratory of Transportation Internet of Things, School of Computer Science and Artificial Intelligence, Wuhan University of Technology, Wuhan 430070, China, and with the State Key Laboratory of Maritime Technology and Safety, Wuhan University of Technology, Wuhan 430063, China (email: zhongx@whut.edu.cn).

Feifei Zhang is with the School of Computer Science and Engineering, Tianjin University of Technology, Tianjin 300382, China (email: feifeizhang@email.tjut.edu.cn).

Rubing Huang is with the School of Computer Science and Engineering, Macau University of Science and Technology, Taipa, Macau 999078, China; and with the Macau University of Science and Technology Zhuhai MUST Science and Technology Research Institute, Zhuhai, Guangdong 519099, China (email: rbhuang@must.edu.mo).

Chia-Wen Lin is with the Department of Electrical Engineering, National Tsing Hua University, Hsinchu 30013, Taiwan (email: cwlin@ee.nthu.edu.tw).

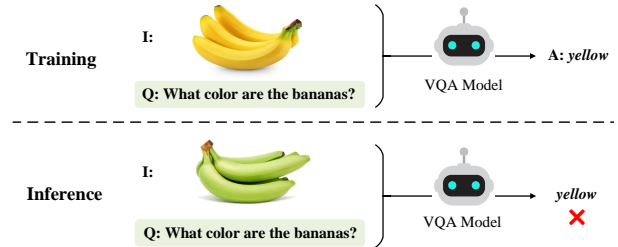


Fig. 1. Illustration of Language Bias. VQA models often exploit superficial correlations between questions and answers, neglecting the image content during inference.

I. INTRODUCTION

VISION-language tasks serve as representative benchmarks for evaluating models’ capabilities in multi-modal learning and visual-linguistic understanding, including visual storytelling [1], video captioning [2], [3], and Visual Question Answering (VQA) [4]. As one of the most essential vision-language tasks, VQA, where an image is accompanied by a natural language question, has attracted considerable attention in recent years due to its requirement for generating accurate natural language responses. This growing interest reflects a shift in the image processing community from conventional “bucketed” recognition toward addressing more intricate multi-modal challenges [4], [5]. Nevertheless, language bias remains a significant challenge in this field. For instance, as illustrated in Fig. 1, the dominant answer for the question type “What color ... bananas?” in the training data is “yellow”. Consequently, VQA models may exploit this simple correlation, relying on superficial cues rather than integrating visual information to capture underlying semantics and perform reasoning, which can lead to incorrect answers.

To address these issues, existing studies have pursued various strategies to mitigate bias. Some researchers have focused on constructing more balanced training datasets to alleviate strong correlations between questions and answers (e.g., correlating “Is there ...?” with “yes”, “What color is ...?” with “black”, and “How many ...?” with “2”) [4], [5]. Others have developed sophisticated architectures that weaken these correlations by incorporating auxiliary branches (e.g., a question-only model), additional objectives, or enhanced visual grounding via refined attention maps [6], [7], [8], [9]. Additionally, several studies have adopted optimization strategies or data augmentation methods during training to prevent models from learning superficial correlations [10], [11], [12], [13].

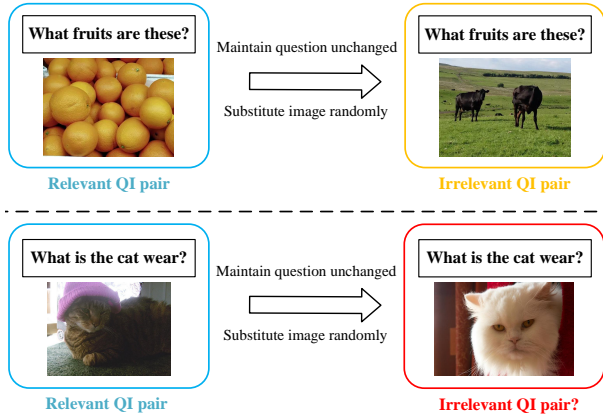


Fig. 2. **Illustration of Existing Approach for Generating Irrelevant QI Pairs.** Although designed to produce irrelevant pairs, this method is flawed: as shown in the bottom row, both images contain a cat while the question pertains to a cat, rendering the generated pair relevant.

Recent studies have extended bias research beyond unimodal contexts. For instance, Zhang *et al.* [14] enhanced multiple-choice Video-QA accuracy by mitigating vision-answer bias, while Vosoughi *et al.* [15] explored additional modalities of bias, proposing a training strategy based on causal inference to reduce multi-modal bias. Moreover, debiasing is crucial in other vision tasks; for example, reducing statistical bias in covariance estimation significantly improves the accuracy of 3D reconstruction [16], and enhancing visual feature learning benefits relation prediction in scene graph generation (SGG) models [17]. These findings underscore the constructive role of debiasing research in advancing the field of vision.

In vision-language tasks, effective question-image (QI) relation learning is critical for high model performance, whereas irrelevant QI inputs can adversely affect predictions. To encourage models to learn authentic QI relations and avoid reliance on superficial correlations, existing methods generate irrelevant QI pairs by randomly substituting the image while keeping the question unchanged. In doing so, the model simultaneously learns the genuine QI correlation from the original pair and the superficial correlation from the generated pair, guided by an appropriate loss function. However, this approach may inadvertently produce QI pairs that remain relevant. As illustrated in Fig. 2, the bottom row shows both images containing a cat while the question pertains to the cat; thus, the generated QI pair is not truly irrelevant, which may adversely affect subsequent learning.

For relevant inputs, the model can correctly infer the answer based on both the image content and the question’s meaning. In contrast, when presented with an irrelevant QI pair, the model may be misled by mismatched information, leading to incorrect answers. As shown in Fig. 3, the relevant input (top instance) provides multi-modal information that facilitates correct reasoning, whereas the irrelevant input (bottom instance) offers unrelated cues that misguide the prediction. If the model refrains from answering irrelevant QI pairs, the overall error rate can be significantly reduced, thereby enhancing its robustness when encountering abnormal inputs. However, no debiasing study has yet addressed the identification of the relevance

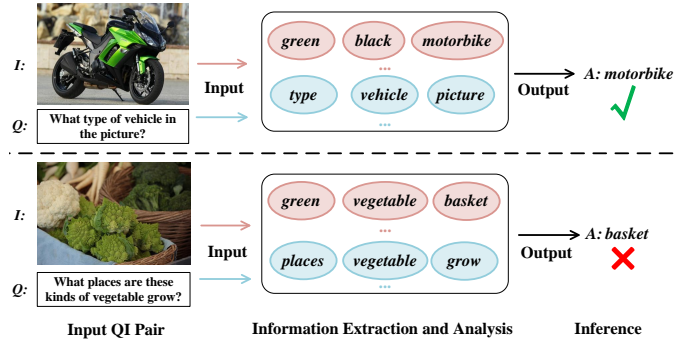


Fig. 3. **Influence of Relevant and Irrelevant QI Pairs on Predictions.** The top instance represents a relevant QI pair, whereas the bottom instance represents an irrelevant QI pair. The red ellipse denotes visual information, and the blue ellipse denotes semantic information. Note that the information extraction and analysis depicted here is schematic and does not reflect the model’s actual operation.

degree of QI inputs.

Moreover, although large language models (LLMs) are increasingly used in vision-language tasks, particularly in Knowledge-based VQA (KBVQA) [18], [19], they do not address language bias in VQA. Recent studies [20], [21], [22] have demonstrated that VQA methods employing LLMs, Pre-trained Language Models (PLMs), and Vision-Language Pre-trained models (VLPs) still suffer from language bias because their training relies on biased data. Consequently, pre-trained large models offer limited benefits for debiasing efforts due to their inherent bias. Additionally, compared to conventional VQA methods, approaches using large models require substantial computational resources, rendering them less suitable for deployment in environments with limited computing capabilities.

Motivated by these challenges, we posit that 1) refined QI relation learning can enhance model performance, and 2) filtering irrelevant QI pairs before prediction can improve model robustness. Accordingly, we propose Optimized Question-Image Relation Learning (QIRL), a generation-based self-supervised learning framework designed to strengthen QI relation learning via a fresh sample generation manner to produce more contrastive samples during the training and a novel identification module for filtering unrelated QI pairs before the model’s inference.

Specifically, we introduce a Negative Image Generation (NIG) module that produces irrelevant QI pairs without human supervision, and an Irrelevant Sample Identification (ISI) module that enables VQA models to handle inputs that do not correspond to relevant QI pairs. The NIG module consists of two components: a diffusion model that converts the original image into a textual description, and an unsupervised sentence revision tool that transforms this description into a negative sentence. This negative sentence is then input to the diffusion model to generate a new image, yielding a QI pair that is markedly different from the original. The ISI module serves as a discriminator between common and irrational QI pairs, and is trained jointly with the VQA model using both original and generated QI pairs. After training, the module directs the

model either to produce a prediction for a common QI pair or to output “abstain” when presented with an irrational QI pair.

Our key contributions can be summarized in threefold:

- We design a novel generation approach for producing highly irrelevant QI pairs within a self-supervised framework for enhancing the model’s QI learning from an absolute contrastive sample perspective.
- We propose an identification module to distinguish between relevant and irrelevant inputs in inference, significantly enhancing the model’s robustness by isolating the adverse effect from unmatched inputs on accuracy.
- Extensive experiments on VQA-CPv2 and VQA-v2 datasets with various base VQA models demonstrate the notable generalizability of the proposed method. Besides, our method achieves performance comparable to state-of-the-art approaches.

II. RELATED WORK

A. Visual Question Answering

Given an image and a natural language question, Visual Question Answering (VQA) [4] requires a system to provide an accurate natural language response. VQA is widely recognized as a benchmark for evaluating models’ capabilities in multimodal learning and visual-linguistic understanding. In recent years, with the advancement of LLMs, Knowledge-Based VQA (KBVQA) [20], [23], [24], [25] has emerged as a popular task that leverages the extensive knowledge of these models to address more challenging questions. Although large models demonstrate notable performance in VQA, they still suffer from language bias inherited from their training data. In this work, we aim to alleviate language bias in VQA models by optimizing question-image (QI) relation learning and introducing an innovative module to detect and filter irrelevant inputs, thereby enhancing model robustness.

B. Debiasing Methods for VQA

Language bias, arising when the answer distribution in the training set differs from that in the test set, remains a critical issue in VQA. Over the past years, numerous debiasing methods have been proposed, which can be broadly categorized into five groups. The first category comprises methods that employ novel model architectures [6], [8], [26], [27]. The second includes approaches that enhance the language model (LM) [28], [29]. The third focuses on methods that improve visual attention mechanisms [9], [30], [31]. The fourth consists of ensemble methods [32], [33], [34], [35], [36], including recent works that use loss estimation scheme [37], adversarial networks [38], margin losses [39], and causal inference [40] to diminish bias. The fifth category involves data-driven strategies [10], [11], [12], [13], [41].

These contributions have significantly advanced debiasing research. Notably, Zhu *et al.* [42] introduced a self-supervised debiasing method that pioneered the use of self-supervised strategies in VQA debiasing, and Cao *et al.* [43] later proposed a robust VQA method based on this approach by integrating contrastive learning and designing a novel loss function.

However, none of these methods generate highly irrelevant samples, and as a result, the QI correlation learning mechanisms remain insufficiently effective. In addition, recent work [20], [21], [22] on debiasing and robustness for VQA methods using pre-trained large models has pointed out that LLMs, PLMs, and VLPs also endure language bias and lack robustness when handling out-of-distribution data. Given these challenges and the deployment difficulties of large models, we focus on a lightweight yet efficient data strategy for boosting VQA performance. In this work, we enhance QI relation learning with a novel generation-based strategy that employs a diffusion model and a sentence revision tool to automatically produce highly contrasting samples.

C. Self-supervised Learning

Self-supervised learning generates supervisory signals directly from the input data, enabling the extraction of high-level representations for various downstream tasks, such as image augmentation [44]. This paradigm has demonstrated success in representation and visual feature learning within computer vision [45]. With recent progress in self-supervised and deep learning, these techniques have also been effectively applied to multimodal domains. In our work, we propose an innovative self-supervised scheme to further advance debiasing and robustness in VQA.

III. PROPOSED METHOD

A. Optimized QI Learning

QI correlation learning is critical for VQA tasks, as the input QI pairs significantly influence model predictions. Since models tend to produce incorrect answers when provided with non-matching (irrelevant) QI inputs, thereby, we propose an optimized QI correlation learning scheme. To encourage the VQA model to learn authentic QI relations from relevant pairs and prevent it from acquiring superficial correlations from irrelevant ones, we devise a highly negative sample generation strategy that utilizes a sentence revision tool and a diffusion model. As training progresses, the loss functions guide the model to rely on relevant QI pairs, and due to the high irrelevance between the generated questions and images, the effectiveness of QI relation learning is further enhanced.

B. Architecture

The architecture of the proposed method is illustrated in Fig. 4 and comprises three main components: the VQA model, the generation of QI pairs, and QI correlation learning. The VQA model is responsible for making predictions based on the inputs. The second component focuses on improving the quality of generated QI pairs to ensure high irrelevance, while the third component promotes VQA performance by alleviating language bias and enhancing model capacity. These components jointly achieve debiasing and robustness promotion through the integration of the Negative Image Generation (NIG) module and the Irrelevant Sample Identification (ISI) module.

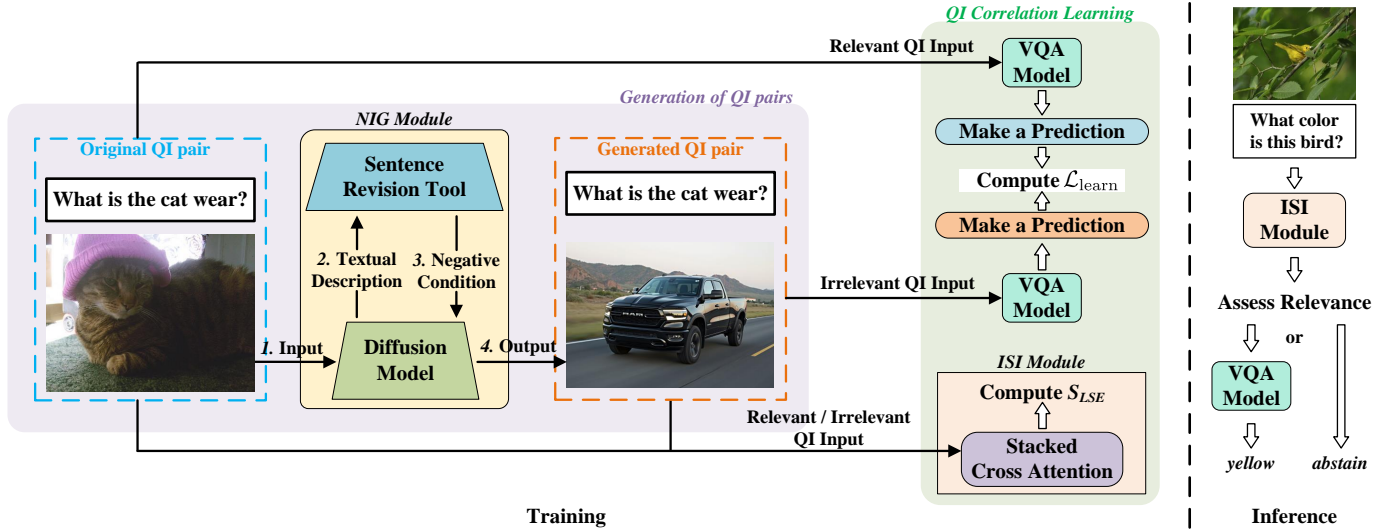


Fig. 4. **Proposed QIRL Architecture Comprises Three Components:** a VQA model, a Generation of QI Pairs module, and a QI Correlation Learning module. The VQA model produces predictions based on the inputs; the Generation of QI Pairs process (purple zone) enhances the quality of generated QI pairs by ensuring they are highly irrelevant; and the QI Correlation Learning process (aqua zone) improves VQA performance by alleviating language bias and increasing model capacity.

1) *VQA Model*: A VQA system, denoted by F , takes an image and a free-form, open-ended natural language question as input and produces a natural language answer [4]. Typically, the VQA problem is formulated as a multi-class classification task. In this formulation, an image I is processed by a convolutional neural network (CNN), and a question Q is processed by a language module. The image and question are then jointly mapped to candidate answers A [46], and the objective is to predict an answer \hat{a} from all candidate answers a based on the image content and question context. Without loss of generality, a VQA model can be formulated as a function transformation:

$$\hat{a} = \arg \max_{a \in A} p(a | Q, I; \theta), \quad (1)$$

where θ denotes the model parameters. A common approach to predict the answer is via the cross-entropy loss, as shown in Eq. (2), or using a multi-label soft loss, as shown in Eq. (3):

$$\mathcal{L}_{ce} = -\frac{1}{N} \sum_{i=1}^N a_i \log p_i, \quad p_i = \text{softmax}(Wh_i + b), \quad (2)$$

where N is the number of samples, and W and b are learnable parameters, with h_i representing the fused multi-modal feature.

$$\mathcal{L}_{ml} = -\frac{1}{N} \sum_{i=1}^N \left[t_i \log \delta(F(A | I_i, Q_i)) + (1 - t_i) \log (1 - \delta(F(A | I_i, Q_i))) \right], \quad (3)$$

where $\delta(\cdot)$ is the sigmoid function and t_i is the soft target score for candidate answer a .

2) *Generation of QI Pairs*: As illustrated in Fig. 3, this component consists of a diffusion model and a sentence simplification tool. Considering the strong cross-modal conversion capabilities of Versatile Diffusion (VD) [47], we employ it for both image-to-text and text-to-image generation. To restrict the content of generated images and avoid similarities to the

original image, we utilize an unsupervised revision manner [48] to produce condition sentences. Initially, the original image of the input QI pair is sent to VD to generate a caption. This caption is then converted into a negative caption through sentence editing, which serves as the condition for new image generation. By introducing a negative condition, the newly generated image becomes highly irrelevant to the original question. Compared with existing methods that randomly substitute the original image from the dataset, our process is more accurate and effective.

3) *QI Correlation Learning*: Following the approach in [42], this component trains the model to estimate the relevance of QI pairs and encourages it to become independent of superficial correlations, thereby alleviating language bias. Specifically, the original QI pair is labeled as relevant ($c = 1$), while the generated QI pair is labeled as irrelevant ($c = 0$). The loss for QI correlation learning, $\mathcal{L}_{\text{learn}}$, is defined as:

$$\mathcal{L}_{\text{learn}} = -\frac{1}{2N} \sum_{i=1}^{2N} \left[c_i \log P(A_i | I_i, Q_i) + \phi(1 - c_i) \log (1 - P(A_i | I_i, Q_i)) \right], \quad (4)$$

where ϕ is a hyper-parameter.

Despite this training scheme reducing reliance on superficial QI correlations, the model may still produce incorrect predictions when faced with irrelevant QI inputs during inference. To address this, we introduce the ISI module to enhance the robustness of the VQA model. Using stacked cross attention [49], the ISI module estimates the similarity S_{LSE} of QI pairs during training and inference, it determines whether the VQA model should provide a prediction or abstain.

C. Negative Image Generation

The NIG module comprises VD [47] and a sentence revision tool [48], where VD is responsible for cross-modal conversion

and the sentence revision tool handles sentence paraphrasing.

The basic processes of VD are similar to conventional diffusion models. Specifically, the forward diffusion process $q(x_T | x_0)$ degrades the data from x_0 to x_T by adding random Gaussian noise. Diffusion models are trained to reverse this process and reconstruct x_0 from x_T by removing the noise; this reverse process $p(x_0 | x_T)$ is defined as a Markov chain [50] with learned Gaussian transitions starting from $p(x_T) = N(x_T; 0, I)$, as shown:

$$\begin{aligned} p_\theta(x_0 | x_T) &= p(x_T) \prod_{t=1}^T p_\theta(x_{t-1} | x_t), \\ p_\theta(x_{t-1} | x_t) &= \mathcal{N}(x_{t-1}; \mu(x_t, t), \Sigma(x_t, t)). \end{aligned} \quad (5)$$

VD's forward diffusion process is similarly defined. The forward process from x_0 to x_T over T steps, with random Gaussian noise added according to a variance schedule β_1, \dots, β_T , is given by:

$$\begin{aligned} q(x_T | x_0) &= \prod_{t=1}^T q(x_t | x_{t-1}), \\ q(x_t | x_{t-1}) &= \mathcal{N}(x_t; \sqrt{1 - \beta_t}x_{t-1}, \beta_t I). \end{aligned} \quad (6)$$

Note that the VD's architecture is multiple flows. Benefiting from its peculiar multi-flow framework, VD can handle various unimodal and multimodal tasks such as image variation, text variation, text-to-image, and image-to-text conversion. In this work, we integrate VD into our framework and use pre-trained four-flow weights for image-to-text and text-to-image conversion in NIG module.

The unsupervised sentence simplification approach [48] is guided by a scoring function that evaluates fluency, simplicity, and meaning preservation. Initially, candidate sentences are generated through a series of lexical and syntactic operations, and an appropriate scoring function is defined to evaluate them. To produce the contrary sentences, we compute a score for each candidate sentence \tilde{s} as follows:

$$f(\tilde{s}) = \frac{f_{\text{LM}}(\tilde{s})^\alpha}{f_{\text{SeI}}(\tilde{s})^\beta f_{\text{SyI}}(\tilde{s})}, \quad (7)$$

where $f_{\text{LM}}(\tilde{s})^\alpha$ measures language fluency using a probabilistic language model [51]; $f_{\text{SeI}}(\tilde{s})^\beta$ measures semantic integrity via cosine similarity; and $f_{\text{SyI}}(\tilde{s})$ assesses syntactic integrity using root tags. The hyper-parameters α and β determine the relative importance of the LM score and semantic integrity, respectively.

Semantic and syntactic integrity indicate the similarity and preservation of content relative to the original sentence; thus, candidate sentences that are more similar to the original receive lower scores. As illustrated in Fig. 5, a constituency parse tree is used to detect phrases (with tags such as S , N , CC , NP , VP , PRP , VBD , D , $ADJP$, and JJ). Unlike the original approach that employs multiple operations (*i.e.*, Removal, Extraction, Reordering, and Substitution), we only perform Removal and Substitution to generate candidate sentences. After sentence editing and score computation, the candidate sentence with the highest score is next selected as the negative condition C_n for VD's image generation.

As shown in Fig. 6, the NIG module involves three steps: **Image-to-Text Conversion:** The original image is converted to a caption by VD, which serves as input to the sentence revision module. **Sentence Paraphrasing:** The caption is edited through

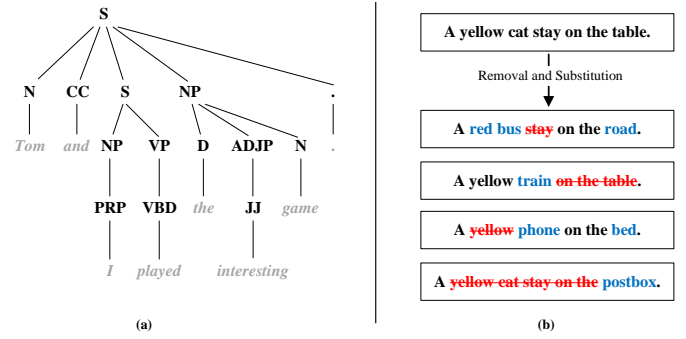


Fig. 5. **Sentence Revision Process.** (a) depicts a parse tree for phrase detection; (b) illustrates two operations used to generate candidate sentences, where the blue words and the red words represent the Substitution operation and the Removal operation, respectively.

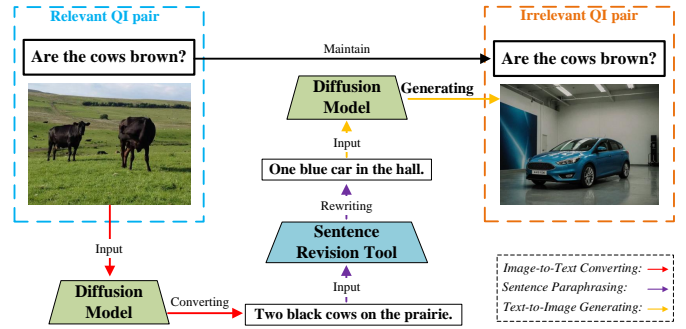


Fig. 6. **NIG Procedure.** First, the original image is converted into a caption by VD, which serves as input to the sentence revision module; next, the caption is negatively paraphrased to produce a revised sentence; finally, VD generates a new image based on this revised sentence. This process yields a negative sample comprising the new image paired with the original question.

negative paraphrasing, and the resulting sentence is used for image generation. **Text-to-Image Generation:** VD generates a new image based on the edited sentence. After this process, a negative sample is produced, comprising the new image paired with the original question.

D. Irrelevant Sample Identification

The ISI module functions as a discriminator that determines whether QI inputs are common (relevant) or not. As illustrated in Fig. 7, the ISI module is trained jointly with the VQA model during the QI correlation learning phase. During training, it learns to compute a matching degree m for the input QI pair and establishes a relation between the relevance label c and m . During inference, the ISI module discriminates whether the input is common or not. As shown in Eq. (8), during inference the ISI module j , the selection function decides whether the VQA model f should provide an answer or abstain:

$$o(x) = (f, j)(x) = \begin{cases} f(x) & \text{if } j(x) = 1, \\ \emptyset & \text{if } j(x) = 0, \end{cases} \quad (8)$$

where the discriminator $j(x)$ is defined based on a threshold γ :

$$j(x) = \begin{cases} 1 & \text{if } j'(x) \geq \gamma; \\ 0 & \text{if } j'(x) < \gamma, \end{cases} \quad (9)$$

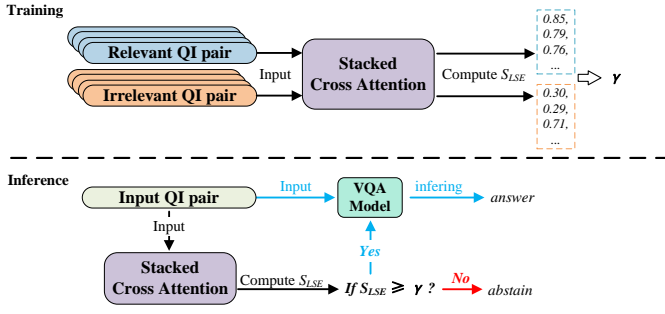


Fig. 7. **Illustration of the ISI module.** During training, the module computes the QI similarity, S_{LSE} , for both relevant and irrelevant QI pairs and determines a threshold γ . During inference, QI pairs are first evaluated based on their similarity scores; pairs scoring below γ are not passed to the VQA model and yield an output of “abstain”, whereas pairs scoring above γ are forwarded to the VQA model for answer prediction.

and $j'(x) : x \rightarrow [0, 1]$ predicts a similarity score that determines whether f should yield an answer.

We use stacked cross attention [49] to compute the matching degree (relevance level) of QI pairs. The training process consists of three steps: Feature encoding, attention to words, and attention to image regions.

1) *Feature Encoding*: The input image I and question Q are encoded into a set of image features $V = (v_1, v_2, \dots, v_n)$, with each v_i representing an image region, and a set of word features $E = (e_1, e_2, \dots, e_m)$, where each e_j encodes a word from the question. These features are obtained using UpDn [26] for the image and an LSTM [52] for the question. The cosine similarity s_{ij} between each image feature v_i and word feature e_j is computed as:

$$s_{ij} = \frac{v_i^T e_j}{\|v_i\| \|e_j\|}, \quad i \in [1, n], j \in [1, m]. \quad (10)$$

2) *Attention to Words*: Attention is imposed on the words for each image region. The attended sentence vector a_i^t for the i^{th} image region is defined as:

$$\begin{aligned} a_i^t &= \sum_{j=1}^m \xi_{ij} e_j, \\ \xi_{ij} &= \frac{\exp \lambda_1 s_{ij}}{\sum_{j=1}^m \exp \lambda_1 s_{ij}}, \end{aligned} \quad (11)$$

where λ_1 is the inverse temperature parameter of the softmax function, and ξ_{ij} represents a variant of dot product attention.

3) *Attention to Image Regions*: The relevance between the i^{th} image region and the sentence is measured by the cosine similarity between the image feature v_i and its corresponding attended sentence vector a_i^t :

$$R(v_i, a_i^t) = \frac{v_i^T a_i^t}{\|v_i\| \|a_i^t\|}, \quad i \in [1, n]. \quad (12)$$

The overall similarity between image I and question Q is then calculated using LogSumExp pooling:

$$S_{LSE}(I, Q) = \log \left(\sum_{i=1}^n \exp \lambda_2 R(v_i, a_i^t) \right)^{\frac{1}{\lambda_2}}, \quad (13)$$

where λ_2 is a parameter that controls the amplification of the most relevant feature pairs.

The hinge-based triplet ranking loss is used as the objective for image-text matching with margin ξ . As shown in Eq. (14), the first term sums over all negative questions \hat{Q} for a given image I , while the second term sums over all negative images \hat{I} for a given question Q . If I and Q are closer in the joint embedding space than any negative pair by a margin ξ , the hinge loss becomes zero.

$$\begin{aligned} L(I, Q) &= \sum_{\hat{Q}} \left[\xi - S_{LSE}(I, Q) + S_{LSE}(I, \hat{Q}) \right]_+ \\ &+ \sum_{\hat{I}} \left[\xi - S_{LSE}(I, Q) + S_{LSE}(\hat{I}, Q) \right]_+, \end{aligned} \quad (14)$$

where $[x]_+ \equiv \max(x, 0)$.

After training, the threshold γ is chosen based on the overlapping region of similarity scores for relevant ($c = 1$) and irrelevant ($c = 0$) QI pairs.

IV. EXPERIMENTAL RESULTS

A. Environment Setup

1) *Datasets and Metrics*: We evaluate the proposed method on two widely used benchmarks: VQAV2 [5] and VQA-CPV2 [6]. VQAV2 is extensively used for training and evaluating VQA models and comprises 265,016 images, including both COCO images and abstract scenes. The COCO images provide rich visual information from real-world environments, featuring diverse objects, scenes, and activities that underpin the associated questions and answers. In contrast, VQA-CPV2 dataset is derived by rearranging the training and validation splits of VQAV2 so that the relation between question types and correct answers differs across the splits. This variation creates a more challenging and realistic evaluation setting, offering insights into the limitations and potential improvements of VQA models.

In our experiments, we employ two metrics. The first is the standard VQA evaluation metric [4], [5], where each predicted answer a is computed as in Eq. (15). In this metric, each question is answered by ten annotators, and the score accounts for discrepancies in human responses.

$$\text{Acc} = \min \left(1, \frac{\# \text{ humans that provide answer } a}{3} \right). \quad (15)$$

The second is a specialized metric designed to assess the performance of the ISI module on irrelevant QI pairs. Under this metric, the predicted answer a is computed as in Eq. (16):

$$\text{Acc}_{\text{spe}}(x) = \begin{cases} \text{Acc}, & \text{if } a \neq \text{abstain}; \\ 1, & \text{if } a = \text{abstain}. \end{cases} \quad (16)$$

In other words, while the standard metric treats an “abstain” response as incorrect (due to the lack of annotation), the specialized metric regards it as correct, thereby evaluating the selective mechanism’s effectiveness.

2) *Implementation Details*: We follow the implementation and training schedule of previous work [42]. In our main experiments, we adopt UpDn [26] and LMH [32] for VQA inference, and employ the multi-label soft loss as the VQA loss. For visual data processing, we utilize pre-trained four-flow

TABLE I
PERFORMANCE COMPARISON ON VQA-CPV2 TEST SET AND VQAV2 VALIDATION SET. Y/N, NUM, AND OTHERS DENOTE THREE DIFFERENT QUESTION TYPES. THE BEST RESULTS ARE HIGHLIGHTED IN BOLD.

Method	Venue	VQA-CPV2				VQAV2			
		Y/N-CP	Num-CP	Others-CP	Overall-CP	Y/N	Num	Others	Overall
<i>Basic Methods</i>									
SAN [27]	CVPR'16	38.35	11.14	21.74	24.96	70.06	39.28	47.84	52.41
GVQA [6]	CVPR'18	57.99	13.68	22.14	31.30	72.03	31.17	34.65	48.24
UpDn [26]	CVPR'18	42.27	11.93	46.05	39.74	81.18	42.14	55.66	63.48
S-MRL [8]	NeurIPS'19	42.85	12.81	43.20	38.46	41.96	12.54	41.35	37.13
<i>Methods with Improved LM</i>									
DLR [28]	AAAI'20	70.99	18.72	45.57	48.87	76.82	39.33	48.54	57.96
VGQE [29]	ECCV'20	66.35	27.08	46.77	50.11	-	-	-	64.04
<i>Methods with Enhanced Visual Attention</i>									
HINT [9]	ICCV'19	67.27	10.61	45.88	46.73	81.18	42.99	55.56	63.38
SCR [30]	NeurIPS'19	70.41	10.42	47.29	48.47	78.80	41.60	54.50	62.20
AttReg [31]	TOMM'22	86.80	51.37	48.25	60.00	79.66	41.68	55.42	62.63
<i>Ensemble Methods</i>									
AdvReg [7]	NeurIPS'18	65.49	15.48	35.48	41.17	79.84	42.35	55.16	62.75
RUBi [8]	NeurIPS'19	68.65	20.28	43.18	47.11	-	-	-	-
LMH [32]	EMNLP'19	70.29	44.10	44.86	52.15	65.06	37.63	54.69	56.35
AdaVQA [36]	IJCAI'21	70.83	49.00	46.29	54.02	47.78	34.13	51.14	46.98
CF-VQA [33]	CVPR'21	90.61	21.50	45.61	55.05	81.13	43.86	50.11	60.94
IntroD [34]	NeurIPS'21	90.79	17.92	46.73	55.17	82.48	46.60	54.05	63.40
GGE [35]	ICCV'21	87.04	27.75	49.59	57.32	73.27	39.99	54.39	59.11
CI-VQA [37]	TIP'22	72.78	48.00	44.31	53.22	68.16	36.35	51.26	56.70
GenB [38]	CVPR'23	88.03	40.05	49.25	59.15	-	-	-	-
RMLVQA [39]	CVPR'23	89.98	45.96	48.74	60.41	76.68	37.54	53.26	59.99
DCCE [40]	EMNLP'24	90.66	45.73	46.03	58.70	77.51	40.26	53.16	60.43
<i>Methods with Data Strategy</i>									
LMH [32] w/ CSS [11]	CVPR'20	84.37	49.42	48.21	58.95	73.25	39.77	55.11	59.91
LMH [32] w/ CSSCL [13]	EMNLP'20	86.99	49.89	47.16	59.18	67.27	38.40	54.71	57.29
LMH [32] w/ QIRL (Ours)		88.22 (↑ 17.93)	51.07 (↑ 6.97)	50.68 (↑ 5.82)	60.03 (↑ 7.88)	82.52 (↑ 17.46)	45.66 (↑ 8.03)	57.42 (↑ 2.73)	64.16 (↑ 7.81)
UpDn [26] w/ CVL [10]	CVPR'20	45.72	12.45	48.34	42.12	-	-	-	-
UpDn [26] w/ RandImg [53]	NeurIPS'20	83.89	41.60	44.20	55.37	76.53	33.87	48.57	57.24
UpDn [26] w/ SSL [42]	IJCAI'20	86.53	29.87	50.03	57.59	-	-	-	63.73
UpDn [26] w/ MUTANT [12]	EMNLP'20	88.90	49.68	50.78	61.72	82.07	42.52	53.28	62.56
UpDn [26] w/ Unshuffling [54]	ICCV'21	47.72	14.43	47.24	42.39	78.32	42.16	52.81	61.08
UpDn [26] w/ D-VQA [41]	NeurIPS'21	88.93	52.12	50.30	61.82	82.11	44.01	57.40	63.69
UpDn [26] w/ KDDAug [55]	ECCV'22	86.13	55.08	48.08	60.24	80.55	41.05	55.18	62.86
UpDn [26] w/ QIRL (Ours)		88.91 (↑ 46.64)	51.60 (↑ 39.67)	51.44 (↑ 5.39)	61.73 (↑ 21.99)	82.75 (↑ 1.57)	46.40 (↑ 4.26)	57.69 (↑ 2.03)	64.92 (↑ 1.44)

weights. Regarding hyper-parameters, we set ϕ in L_{learn} to 3; α and β in $f(\hat{s})$ to 0.3 and 1, respectively; and λ_1 in ξ_{ij} and λ_2 in $S_{\text{LSE}}(I, Q)$ to 4 and 5, respectively. During training, the threshold γ in $j(x)$ is fixed at 0.71.

B. Quantitative Results

The main quantitative results are summarized in Table I and Fig. 8. Columns 3 to 6 report results on VQA-CPV2 test set, while columns 7 to 10 present results on VQAV2 validation set. We report accuracies for various question types, namely, yes/no (Y/N), number (Num), and other (Others), as well as overall accuracy.

Compared with baseline models, our method yields remarkable improvements. For the LMH model [32] on VQA-CPV2 test set, our approach improves yes/no accuracy by 17.93%, number accuracy by 6.97%, and other accuracy by

5.82%, resulting in an overall accuracy gain of 7.88% on VQA-CPV2 and 7.81% on VQAV2. For the UpDn model [26], our method enhances yes/no, number, and other accuracies on VQA-CPV2 test set by 46.64%, 39.67%, and 5.39%, respectively, leading to overall accuracy gains of 21.99% on VQA-CPV2 and 1.44% on VQAV2.

Compared with methods based on data strategies, our approach achieves competitive performance across various question types on VQA-CPV2 test set, ranking second in overall accuracy on VQA-CPV2 and first on VQAV2. Note that QIRL's results on VQA-CPV2 are inferior to those of D-VQA [41], which mitigates both language and vision biases. Although D-VQA achieves superior performance, its sophisticated architecture incurs higher training and inference time. Overall, our proposed method outperforms most existing approaches, particularly in overall accuracy, where it attains the best results on both VQA-CPV2 test set and VQAV2

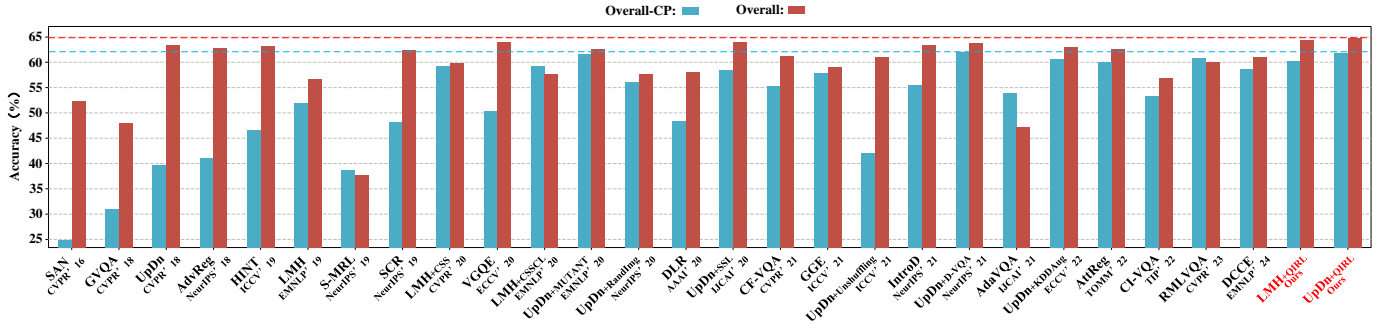


Fig. 8. **Quantitative Analysis of Debiasing Studies.** Blue dashed line and red dashed line in the figure indicate the best result in overall accuracy of VQA-CPV2 TEST SET and VQA2 VALIDATION SET, respectively.

TABLE II

PERFORMANCE COMPARISON OF QIRL AND KBVQA BASELINES ON OKVQA AND VQA-CP TEST SET. NOTE THAT A SPECIALIZED METRIC IS USED TO EVALUATE QIRL SINCE THE KNOWLEDGE-REQUIRED QUESTION-ANSWER FORMAT AFFECTS THE VQA MODEL’S STANDARD INFERENCE.

Method	Venue	OKVQA	VQA-CP
PiCa [23]	AAAI’22	48.06	50.08
KAT [56]	NAACL’22	54.41	51.94
REVIVE [57]	NeurIPS’22	58.03	52.59
PromptCap [24]	ICCV’23	60.47	53.74
Prophet [25]	CVPR’23	61.11	53.41
GRACE [20]	ECCV’24	60.32	57.35
UpDn [26] w/ QIRL (Ours)		60.65	59.11

TABLE III

PERFORMANCE EVALUATION OF DIFFERENT VQA BASELINES ON VQA-CPV2 TEST SET.

Method	Accuracy	Improvement
SAN [27]	24.96	–
SAN [27] w/ SSL [42]	37.64	↑ 12.68
SAN [27] w/ D-VQA [41]	52.17	↑ 27.21
SAN [27] w/ QIRL (Ours)	48.11	↑ 23.15
UpDn [26]	39.74	–
UpDn [26] w/ CSS [11]	41.16	↑ 1.42
UpDn [26] w/ CSSCL [13]	40.38	↑ 0.64
UpDn [26] w/ MUTANT [12]	50.03	↑ 10.29
UpDn [26] w/ SSL [42]	57.59	↑ 17.85
UpDn [26] w/ D-VQA [41]	61.82	↑ 22.08
UpDn [26] w/ KDDAug [55]	60.24	↑ 20.50
UpDn [26] w/ QIRL (Ours)	61.73	↑ 21.99
S-MRL [8]	38.46	–
S-MRL [8] w/ SSL [42]	49.09	↑ 10.63
S-MRL [8] w/ QIRL (Ours)	56.14	↑ 17.68
HINT [9]	46.73	–
HINT [9] w/ SSL [42]	54.96	↑ 8.23
HINT [9] w/ QIRL (Ours)	58.01	↑ 11.28
LMH [32]	52.15	–
LMH [32] w/ CSS [11]	58.95	↑ 6.80
LMH [32] w/ CSSCL [13]	59.18	↑ 7.03
LMH [32] w/ KDDAug [55]	59.54	↑ 7.39
LMH [32] w/ QIRL (Ours)	60.03	↑ 7.88

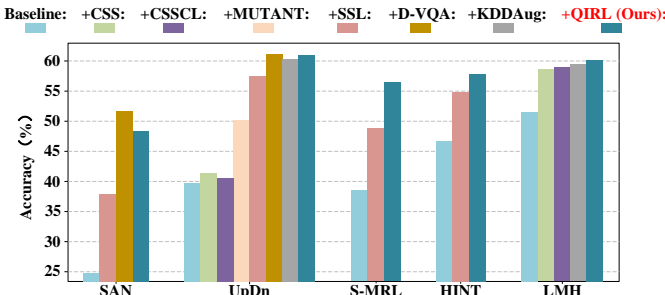


Fig. 9. **Performance Comparison of Data Strategy Methods with Different VQA models.** The methods are illustrated with colored bars.

validation set.

In addition to comparing QIRL with conventional debiasing methods, we also compare the proposed method with KBVQA baselines on OKVQA test set [18] and VQA-CP test set [6]. OKVQA dataset is commonly used for evaluating knowledge-intensive questions, while VQA-CP dataset serves as a standard benchmark for assessing generalization capacity. We adopt the specialized metric for evaluating QIRL, given that the knowledge-required question-answer format influences regular VQA inference. The results in Table II highlight the efficacy of the combined NIG and ISI modules, achieving competitive performance even compared with KBVQA methods employing LLMs.

Further, the results from different VQA baselines on VQA-CPV2 test set are presented in Fig. 9 and Table III (with bold fonts indicating the best results). Although D-VQA achieves the

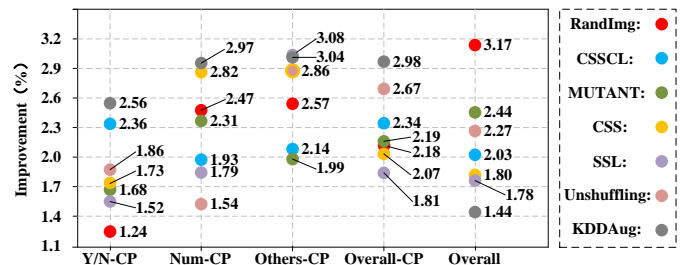


Fig. 10. **Evaluation of the Effectiveness of the ISI Module.** Improvements achieved by the ISI module across various methods are illustrated using different colors.

TABLE IV
PERFORMANCE EVALUATION OF DIFFERENT VQA LOSSES ON VQA-CPV2 TEST SET.

Loss	Method	Data strategy	Y/N	Num	Others	Overall
Cross-Entropy Loss	UpDn [26]	No	47.27	13.67	40.32	38.28
	UpDn [26] w/ QIRL (Ours)	Yes	88.92	50.28	48.70	59.20
Multi-Label Loss	UpDn [26]	No	43.45	13.64	48.18	41.53
	UpDn [26] w/ QIRL (Ours)	Yes	88.91	51.60	51.44	61.73

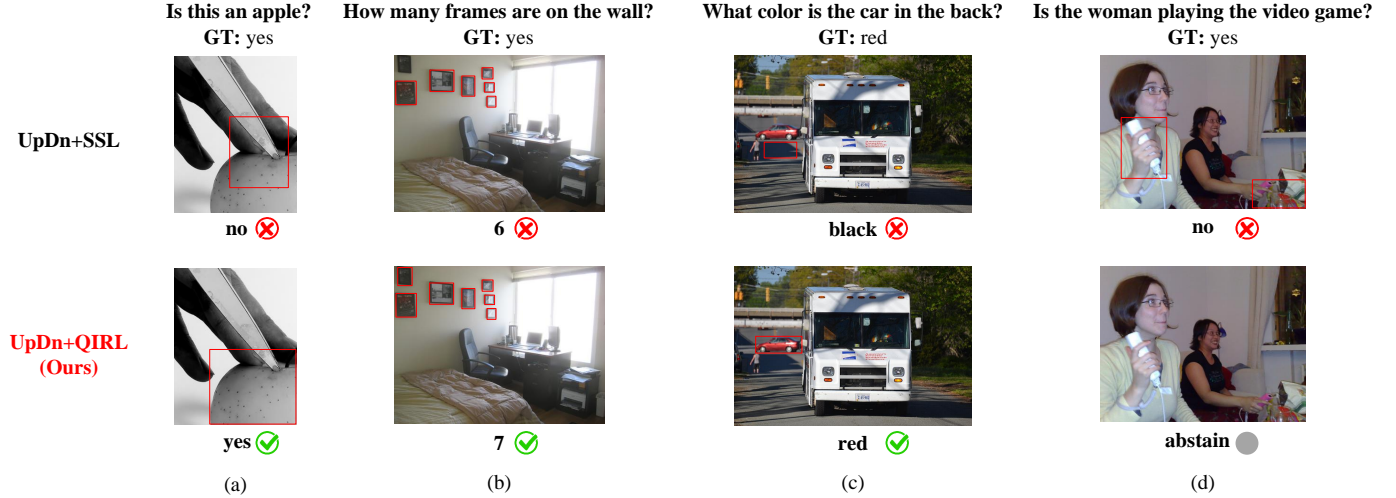


Fig. 11. **Qualitative Analysis.** Red boxes indicate the regions where the methods focus.

TABLE V
COMPARISON OF STANDARD (Acc) AND SPECIALIZED (Acc_{spe}) METRICS ON VQA-CPV2 TEST SET AND VQAV2 VALIDATION SET.

Method	VQA-CPv2				VQAV2
	Y/N-CP	Num-CP	Others-CP	Overall-CP	Overall
QIRL – Acc	88.91	51.60	51.44	61.73	64.92
QIRL – Acc _{spe}	88.93	52.14	56.93	65.03	67.01

best improvements for SAN and UpDn, its approach does not generalize as well to other baselines. In contrast, our method is model-agnostic and can be integrated with various VQA models. Specifically, QIRL improves accuracy by 23.15% for SAN, 21.99% for UpDn, 17.68% for S-MRL, 11.28% for HINT, and 7.88% for LMH. In summary, QIRL achieves competitive results compared with other data strategies, realizing the best or second-best improvement for each VQA baseline.

The performance of our method using different VQA loss functions on VQA-CPv2 test set is summarized in Table IV. We report accuracies for various question types based on two losses: cross-entropy loss and multi-label loss. With cross-entropy loss, our method achieves improvements of 1.17%, 23.88%, and 7.28% for different question types, along with a 6.57% gain in overall accuracy. With multi-label loss, the improvements are 2.38%, 21.73%, and 0.41%, resulting in a 4.14% overall gain.

To evaluate the robustness of the proposed method in handling irrelevant QI pairs, we introduce a specialized metric that treats an “abstain” output as correct, in contrast to the

standard metric [4]. Evaluation on VQA-CPv2 validation set and VQAV2 test set (see Table V) shows a significant improvement in accuracy when an “abstain” response is considered correct, thereby confirming the effectiveness of our selective mechanism.

Moreover, to further validate the ISI module’s effectiveness, we integrate the pre-trained ISI module into other data strategy methods and conduct experiments on VQA-CPv2 test set and VQAV2 validation set. The results, reported in Table VI and illustrated in Fig. 10, indicate that all methods benefit from the integration of the ISI module, with improvements ranging from at least 1.24% up to 3.17% (as observed for RandImg w/ ISI on VQAV2 validation set). These findings clearly demonstrate that the ISI module significantly enhances model robustness for data strategy-based methods.

C. Qualitative Analysis

Qualitative results are presented in Fig. 11, which shows four representative cases comparing predictions from SSL (based on a self-learning strategy) and our method using the UpDn base model. Cases (a) and (d) correspond to yes/no questions, case (b) to a number question, and case (c) to another question. Bounding boxes highlight the image regions that the models focus on. In the first three cases, SSL produces incorrect answers, whereas our method yields correct responses by concentrating on more relevant regions. In case (d), although neither SSL nor our method predicts the correct answer, our selective mechanism allows our method to output “abstain” instead of an incorrect answer.

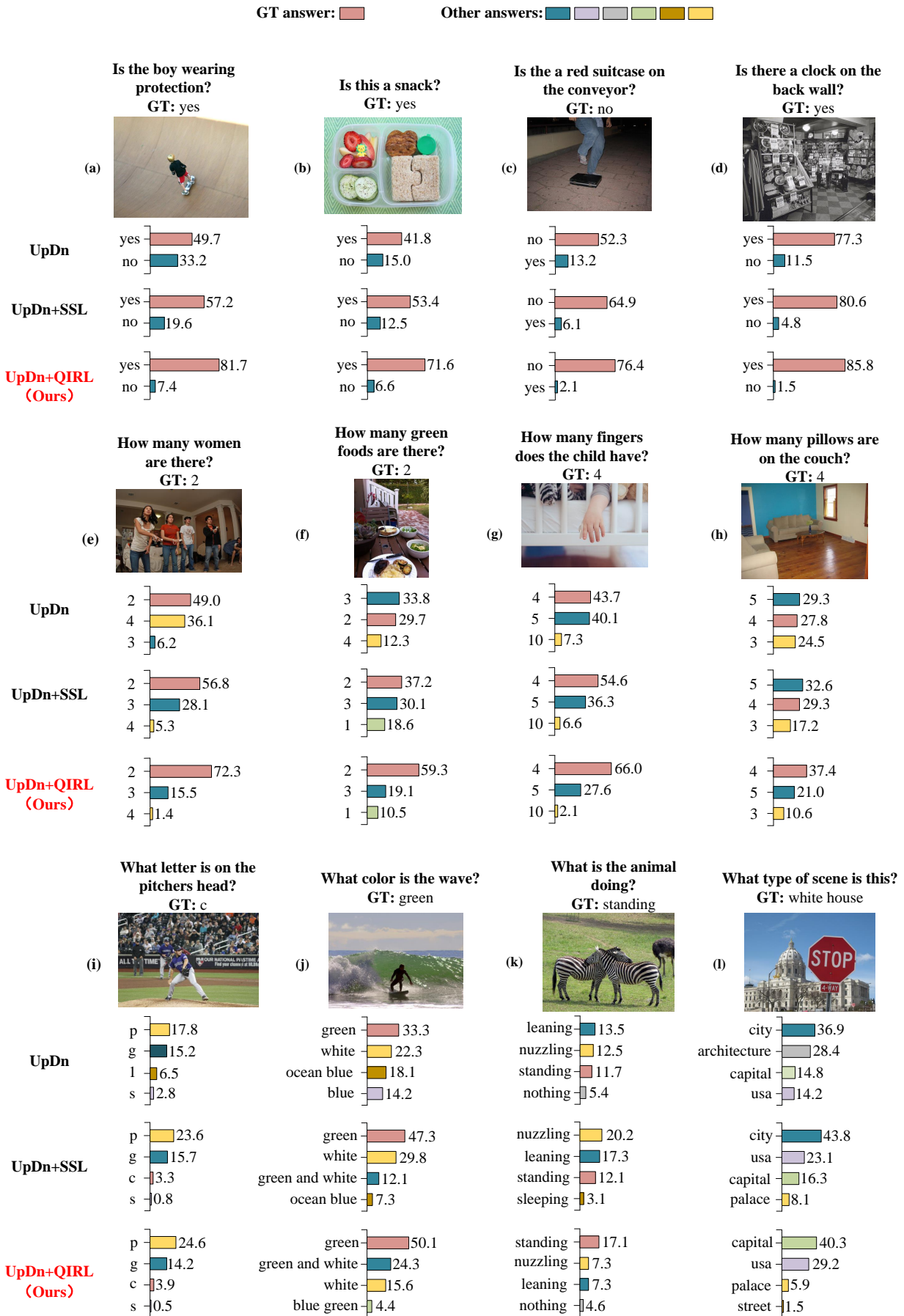


Fig. 12. Qualitative Analysis. The red bar means the probability of the GT answer, and other colored bars represent the probability of others.

TABLE VI
PERFORMANCE COMPARISON OF DATA STRATEGY METHODS AUGMENTED WITH THE ISI MODULE ON VQA-CPV2 TEST SET AND VQAV2 VALIDATION SET. UNSHADED CELLS DENOTE RESULTS FROM METHODS WITHOUT THE ISI MODULE EVALUATED USING THE STANDARD METRIC, WHILE GRAY CELLS INDICATE RESULTS FROM METHODS WITH THE ISI MODULE EVALUATED USING THE SPECIALIZED METRIC.

Baseline	Venue	Method	VQA-CPv2				VQAv2
			Y/N-CP	Num-CP	Others-CP	Overall-CP	Overall
RandImg [53]	NeurIPS'20	Original	83.89	41.60	44.20	55.37	57.24
			85.13 (↑ 1.24)	44.07 (↑ 2.47)	46.77 (↑ 2.57)	57.55 (↑ 2.18)	60.41 (↑ 3.17)
CSSCL [13]	EMNLP'20	Original	86.99	49.89	47.16	59.18	57.29
			89.35 (↑ 2.36)	51.82 (↑ 1.93)	49.30 (↑ 2.14)	61.52 (↑ 2.34)	59.32 (↑ 2.03)
MUTANT [12]	EMNLP'20	Original	88.90	49.68	50.78	61.72	62.56
			90.58 (↑ 1.68)	51.99 (↑ 2.31)	52.77 (↑ 1.99)	63.91 (↑ 2.19)	65.00 (↑ 2.44)
CSS [11]	CVPR'20	Original	84.37	49.42	48.21	58.95	59.91
			86.10 (↑ 1.73)	52.24 (↑ 2.82)	51.07 (↑ 2.86)	61.02 (↑ 2.07)	61.71 (↑ 1.80)
SSL [42]	IJCAI'20	Original	86.53	29.87	50.03	57.59	63.73
			88.05 (↑ 1.52)	31.66 (↑ 1.79)	53.11 (↑ 3.08)	59.40 (↑ 1.81)	65.51 (↑ 1.78)
Unshuffling [54]	ICCV'21	Original	47.72	14.43	47.24	42.39	61.08
			49.58 (↑ 1.86)	15.97 (↑ 1.54)	50.10 (↑ 2.86)	45.06 (↑ 2.67)	63.35 (↑ 2.27)
KDDAug [55]	ECCV'22	Original	86.13	55.08	48.08	60.24	62.86
			88.69 (↑ 2.56)	58.05 (↑ 2.97)	51.12 (↑ 3.04)	63.22 (↑ 2.98)	64.30 (↑ 1.44)

TABLE VII
ABLATION STUDIES ON THE NIG AND ISI MODULES ON VQA-CPV2 TEST SET AND VQAV2 VALIDATION SET.

Method	NIG	ISI	VQA-CPv2				VQAv2
			Y/N-CP	Num-CP	Others-CP	Overall-CP	Overall
UpDn [26]	○	○	42.27	11.93	46.05	39.74	63.48
UpDn [26] w/ QIRL	●	○	88.91	51.60	50.44	61.73	64.92
UpDn [26] w/ QIRL	○	●	86.55	34.72	50.29	59.10	63.91
UpDn [26] w/ QIRL	●	●	88.93	52.14	56.93	65.03	67.01

Moreover, we compare the prediction probabilities corresponding to the answers among the base model, SSL, and our method, as illustrated in Fig. 12. Cases (a)–(d) are yes/no questions; (e)–(h) are number questions; and (i)–(l) are other questions. In the figures, the red bar indicates the probability of the ground truth answer, while the other colored bars represent the probabilities of alternative answers. In most cases, our method not only increases the prediction probability for the correct answer but also reduces the probabilities for incorrect ones. For yes/no questions, our method further improves the probability of the correct answer. For number and other questions, as illustrated in cases (f), (h), (j), and (k), our method assigns the highest probability to the correct answer while suppressing confusion from other answers. Although in cases (i) and (l) none of the methods produces the highest probability for the correct answer, owing to difficulties such as fuzzy target regions or ambiguous image content, our method still demonstrates the best relative performance compared to the base model and SSL.

D. Ablation Studies

To assess the contributions of the proposed NIG and ISI modules, we conduct ablation studies by evaluating our method with and without each module. The results, based on the specialized metric, are reported in Table VII. We consider three variants: one with only the NIG module, one with only the ISI

module (using the SSL sample generation strategy), and one with both modules integrated. The variant with only the NIG module does not produce any “abstain” outputs, yielding results identical to those evaluated with the standard metric. These experiments demonstrate that both the NIG and ISI modules jointly contribute to accuracy improvements and effectively mitigate language bias in VQA.

V. CONCLUSION AND DISCUSSION

In this paper, we propose Optimized Question-Image Relation Learning (QIRL), a generation-based self-supervised framework designed to enhance the robustness of VQA. To improve question-image (QI) correlation learning, we introduce a novel generation strategy that automatically produces highly irrelevant QI pairs. Specifically, a Negative Image Generation (NIG) module is devised to generate these irrelevant QI pairs without human supervision. Furthermore, to boost model robustness, we propose an identification module that assesses input relevance and determines whether the model should yield a prediction or abstain during inference. This Irrelevant Sample Identification (ISI) module guides the VQA system in handling irrational inputs that do not correspond to the intended QI pairs via filtering out this kind of input and outputting “abstain”.

Although our method outperforms the baseline and achieves performance comparable to previous approaches, several limitations remain. First, the evaluation protocol for robustness is not

yet sufficiently comprehensive. Second, while highly irrelevant QI pairs are successfully generated, further exploration of the bias in QI correlation learning is warranted. Finally, given that large models also suffer from similar bias problems, developing debiasing strategies for VQA methods using large models remains a promising topic for future research.

To address these limitations, we propose several avenues for future research: 1) developing a more robust and fair evaluation protocol to better validate the proposed method; 2) extending the debiasing approach from solely addressing language bias to also mitigating vision bias, thereby reducing multi-modal bias; and 3) incorporating debiasing concepts into VQA methods that employ large models to further enhance their robustness. With these improvements, we anticipate further reductions in language bias and significant gains in model robustness.

REFERENCES

- [1] L. Yang, Z. Xiao, W. Huang, and X. Zhong, "StoryLLaVA: enhancing visual storytelling with multi-modal large language models," in *Proceedings of the International Conference on Computational Linguistics*, pp. 3936–3951, 2025.
- [2] X. Zhong, Z. Li, S. Chen, K. Jiang, C. Chen, and M. Ye, "Refined semantic enhancement towards frequency diffusion for video captioning," in *Proceedings of the AAAI Conference on Artificial Intelligence*, pp. 3724–3732, 2023.
- [3] S. Chen, X. Zhong, Y. Zhang, L. Zhu, P. Li, X. Yang, and B. Sheng, "Action-aware linguistic skeleton optimization network for non-autoregressive video captioning," *ACM Transactions on Multimedia Computing, Communications, and Applications*, vol. 20, no. 10, pp. 326:1–326:24, 2024.
- [4] A. Agrawal, J. Lu, S. Antol, M. Mitchell, C. L. Zitnick, D. Parikh, and D. Batra, "VQA: visual question answering - www.visualqa.org," *International Journal of Computer Vision*, vol. 123, no. 1, pp. 4–31, 2017.
- [5] Y. Goyal, T. Khot, A. Agrawal, D. Summers-Stay, D. Batra, and D. Parikh, "Making the V in VQA matter: Elevating the role of image understanding in visual question answering," *International Journal of Computer Vision*, vol. 127, no. 4, pp. 398–414, 2019.
- [6] A. Agrawal, D. Batra, D. Parikh, and A. Kembhavi, "Don't just assume; look and answer: Overcoming priors for visual question answering," in *Proceedings of the IEEE/CVF Conference on Computer Vision and Pattern Recognition*, pp. 4971–4980, 2018.
- [7] S. Ramakrishnan, A. Agrawal, and S. Lee, "Overcoming language priors in visual question answering with adversarial regularization," in *Advances in Neural Information Processing Systems*, pp. 1548–1558, 2018.
- [8] R. Cadène, C. Dancette, H. Ben-Younes, M. Cord, and D. Parikh, "RUBi: reducing unimodal biases for visual question answering," in *Advances in Neural Information Processing Systems*, pp. 839–850, 2019.
- [9] R. R. Selvaraju, S. Lee, Y. Shen, H. Jin, S. Ghosh, L. P. Heck, D. Batra, and D. Parikh, "Taking a HINT: leveraging explanations to make vision and language models more grounded," in *Proceedings of the IEEE/CVF International Conference on Computer Vision*, pp. 2591–2600, 2019.
- [10] E. Abbasnejad, D. Teney, A. Parvaneh, J. Shi, and A. van den Hengel, "Counterfactual vision and language learning," in *Proceedings of the IEEE/CVF Conference on Computer Vision and Pattern Recognition*, pp. 10041–10051, 2020.
- [11] L. Chen, Y. Zheng, Y. Niu, H. Zhang, and J. Xiao, "Counterfactual samples synthesizing and training for robust visual question answering," *IEEE Transactions on Pattern Analysis and Machine Intelligence*, vol. 45, no. 11, pp. 13218–13234, 2023.
- [12] T. Gokhale, P. Banerjee, C. Baral, and Y. Yang, "MUTANT: A training paradigm for out-of-distribution generalization in visual question answering," in *Proceedings of the Conference on Empirical Methods in Natural Language Processing*, pp. 878–892, 2020.
- [13] Z. Liang, W. Jiang, H. Hu, and J. Zhu, "Learning to contrast the counterfactual samples for robust visual question answering," in *Proceedings of the Conference on Empirical Methods in Natural Language Processing*, pp. 3285–3292, 2020.
- [14] X. Zhang, F. Zhang, and C. Xu, "Reducing vision-answer biases for multiple-choice VQA," *IEEE Transactions on Image Processing*, vol. 32, pp. 4621–4634, 2023.
- [15] A. Vosoughi, S. Deng, S. Zhang, Y. Tian, C. Xu, and J. Luo, "Cross modality bias in visual question answering: A causal view with possible worlds VQA," *IEEE Transactions on Multimedia*, vol. 26, pp. 8609–8624, 2024.
- [16] A. K. Roy-Chowdhury and R. Chellappa, "Statistical bias in 3-D reconstruction from a monocular video," *IEEE Transactions on Image Processing*, vol. 14, no. 8, pp. 1057–1062, 2005.
- [17] T. He, L. Gao, J. Song, and Y. Li, "State-aware compositional learning toward unbiased training for scene graph generation," *IEEE Transactions on Image Processing*, vol. 32, pp. 43–56, 2023.
- [18] K. Marino, M. Rastegari, A. Farhadi, and R. Mottaghi, "OK-VQA: A visual question answering benchmark requiring external knowledge," in *Proceedings of the IEEE/CVF Conference on Computer Vision and Pattern Recognition*, pp. 3195–3204, 2019.
- [19] S. Shah, A. Mishra, N. Yadati, and P. P. Talukdar, "KVQA: knowledge-aware visual question answering," in *Proceedings of the AAAI Conference on Artificial Intelligence*, pp. 8876–8884, 2019.
- [20] Y. Zhang, M. Jiang, and Q. Zhao, "GRACE: graph-based contextual debiasing for fair visual question answering," in *Proceedings of the European Conference on Computer Vision*, pp. 176–194, 2024.
- [21] Q. Si, Y. Liu, Z. Lin, P. Fu, Y. Cao, and W. Wang, "Compressing and debiasing vision-language pre-trained models for visual question answering," in *Proceedings of the Conference on Empirical Methods in Natural Language Processing*, pp. 513–529, 2023.
- [22] X. Fu, S. Zhang, G. Kwon, P. Perera, H. Zhu, Y. Zhang, A. H. Li, W. Y. Wang, Z. Wang, V. Castelli, P. Ng, D. Roth, and B. Xiang, "Generate then select: Open-ended visual question answering guided by world knowledge," in *Findings of the Association for Computational Linguistics*, pp. 2333–2346, 2023.
- [23] Z. Yang, Z. Gan, J. Wang, X. Hu, Y. Lu, Z. Liu, and L. Wang, "An empirical study of GPT-3 for few-shot knowledge-based VQA," in *Proceedings of the AAAI Conference on Artificial Intelligence*, pp. 3081–3089, 2022.
- [24] Y. Hu, H. Hua, Z. Yang, W. Shi, N. A. Smith, and J. Luo, "Prompt-Cap: prompt-guided task-aware image captioning," *arXiv preprint arXiv:2211.09699*, 2022.
- [25] Z. Shao, Z. Yu, M. Wang, and J. Yu, "Prompting large language models with answer heuristics for knowledge-based visual question answering," in *Proceedings of the IEEE/CVF Conference on Computer Vision and Pattern Recognition*, pp. 14974–14983, 2023.
- [26] P. Anderson, X. He, C. Buehler, D. Teney, M. Johnson, S. Gould, and L. Zhang, "Bottom-up and top-down attention for image captioning and visual question answering," in *Proceedings of the IEEE/CVF Conference on Computer Vision and Pattern Recognition*, pp. 6077–6086, 2018.
- [27] Z. Yang, X. He, J. Gao, L. Deng, and A. J. Smola, "Stacked attention networks for image question answering," in *Proceedings of the IEEE/CVF Conference on Computer Vision and Pattern Recognition*, pp. 21–29, 2016.
- [28] C. Jing, Y. Wu, X. Zhang, Y. Jia, and Q. Wu, "Overcoming language priors in VQA via decomposed linguistic representations," in *Proceedings of The AAAI Conference on Artificial Intelligence*, pp. 11181–11188, 2020.
- [29] G. KV and A. Mittal, "Reducing language biases in visual question answering with visually-grounded question encoder," in *Proceedings of the European Conference on Computer Vision*, pp. 18–34, 2020.
- [30] J. Wu and R. J. Mooney, "Self-critical reasoning for robust visual question answering," in *Advances in Neural Information Processing Systems*, pp. 8601–8611, 2019.
- [31] Y. Liu, Y. Guo, J. Yin, X. Song, W. Liu, L. Nie, and M. Zhang, "Answer questions with right image regions: A visual attention regularization approach," *ACM Transactions on Multimedia Computing, Communications, and Applications*, vol. 18, pp. 93:1–93:18, 2022.
- [32] C. Clark, M. Yatskar, and L. Zettlemoyer, "Don't take the easy way out: Ensemble based methods for avoiding known dataset biases," in *Proceedings of the Conference on Empirical Methods in Natural Language Processing*, pp. 4067–4080, 2019.
- [33] Y. Niu, K. Tang, H. Zhang, Z. Lu, X. Hua, and J. Wen, "Counterfactual VQA: A cause-effect look at language bias," in *Proceedings of the IEEE/CVF Conference on Computer Vision and Pattern Recognition*, pp. 12700–12710, 2021.
- [34] Y. Niu and H. Zhang, "Introspective distillation for robust question answering," in *Advances in Neural Information Processing Systems*, pp. 16292–16304, 2021.
- [35] X. Han, S. Wang, C. Su, Q. Huang, and Q. Tian, "Greedy gradient ensemble for robust visual question answering," in *Proceedings of the IEEE/CVF International Conference on Computer Vision*, pp. 1564–1573, 2021.

- [36] Y. Guo, L. Nie, Z. Cheng, F. Ji, J. Zhang, and A. D. Bimbo, "AdaVQA: overcoming language priors with adapted margin cosine loss," in *Proceedings of the International Joint Conference on Artificial Intelligence*, pp. 708–714, 2021.
- [37] Y. Guo, L. Nie, Z. Cheng, Q. Tian, and M. Zhang, "Loss re-scaling VQA: revisiting the language prior problem from a class-imbalance view," *IEEE Transactions on Image Processing*, vol. 31, pp. 227–238, 2022.
- [38] J. Cho, D. Kim, H. Ryu, and I. S. Kweon, "Generative bias for robust visual question answering," in *Proceedings of the IEEE/CVF Conference on Computer Vision and Pattern Recognition*, pp. 11681–11690, 2023.
- [39] A. Basu, S. Addepalli, and R. V. Babu, "RMLVQA: A margin loss approach for visual question answering with language biases," in *Proceedings of the IEEE/CVF Conference on Computer Vision and Pattern Recognition*, pp. 11671–11680, 2023.
- [40] L. Song, C. Yang, X. Li, and X. Shang, "A robust dual-debiasing VQA model based on counterfactual causal effect," in *Proceedings of the Conference on Empirical Methods in Natural Language Processing*, pp. 4242–4252, 2024.
- [41] Z. Wen, G. Xu, M. Tan, Q. Wu, and Q. Wu, "Debiased visual question answering from feature and sample perspectives," in *Advances in Neural Information Processing Systems*, pp. 3784–3796, 2021.
- [42] X. Zhu, Z. Mao, C. Liu, P. Zhang, B. Wang, and Y. Zhang, "Overcoming language priors with self-supervised learning for visual question answering," in *Proceedings of the International Joint Conference on Artificial Intelligence*, pp. 1083–1089, 2020.
- [43] R. Cao, Z. Li, Z. Tang, C. Zhang, and H. Ma, "Enhancing robust VQA via contrastive and self-supervised learning," *Pattern Recognition*, vol. 159, 2025.
- [44] D. Pathak, P. Krähenbühl, J. Donahue, T. Darrell, and A. A. Efros, "Context encoders: Feature learning by inpainting," in *Proceedings of the IEEE/CVF Conference on Computer Vision and Pattern Recognition*, pp. 2536–2544, 2016.
- [45] C. Doersch, A. Gupta, and A. A. Efros, "Unsupervised visual representation learning by context prediction," in *Proceedings of the IEEE/CVF International Conference on Computer Vision*, pp. 1422–1430, 2015.
- [46] V. Manjunatha, N. Saini, and L. S. Davis, "Explicit bias discovery in visual question answering models," in *Proceedings of the IEEE/CVF Conference on Computer Vision and Pattern Recognition*, pp. 9562–9571, 2019.
- [47] X. Xu, Z. Wang, E. J. Zhang, K. Wang, and H. Shi, "Versatile diffusion: Text, images and variations all in one diffusion model," in *Proceedings of the IEEE/CVF International Conference on Computer Vision*, pp. 7720–7731, 2023.
- [48] D. Kumar, L. Mou, L. Golab, and O. Vechtomova, "Iterative edit-based unsupervised sentence simplification," in *Proceedings of the Annual Meeting of the Association for Computational Linguistics*, pp. 7918–7928, 2020.
- [49] K. Lee, X. Chen, G. Hua, H. Hu, and X. He, "Stacked cross attention for image-text matching," in *Proceedings of the European Conference on Computer Vision*, pp. 212–228, 2018.
- [50] J. Ho, A. Jain, and P. Abbeel, "Denoising diffusion probabilistic models," in *Advances in Neural Information Processing Systems*, 2020.
- [51] N. Miao, H. Zhou, L. Mou, R. Yan, and L. Li, "CGMH: constrained sentence generation by metropolis-hastings sampling," in *Proceedings of the AAAI Conference on Artificial Intelligence*, pp. 6834–6842, 2019.
- [52] A. Graves and A. Graves, "Long short-term memory," *Supervised sequence labelling with recurrent neural networks*, pp. 37–45, 2012.
- [53] D. Teney, E. Abbasnejad, K. Kafle, R. Shrestha, C. Kanan, and A. van den Hengel, "On the value of out-of-distribution testing: An example of goodhart's law," in *Advances in Neural Information Processing Systems*, 2020.
- [54] D. Teney, E. Abbasnejad, and A. van den Hengel, "Unshuffling data for improved generalization in visual question answering," in *Proceedings of the IEEE/CVF International Conference on Computer Vision*, pp. 1397–1407, 2021.
- [55] L. Chen, Y. Zheng, and J. Xiao, "Rethinking data augmentation for robust visual question answering," in *Proceedings of the European Conference on Computer Vision*, pp. 95–112, 2022.
- [56] L. Gui, B. Wang, Q. Huang, A. Hauptmann, Y. Bisk, and J. Gao, "KAT: A knowledge augmented transformer for vision-and-language," in *Proceedings of the Conference of the North American Chapter of the Association for Computational Linguistics: Human Language Technologies*, pp. 956–968, 2022.
- [57] Y. Lin, Y. Xie, D. Chen, Y. Xu, C. Zhu, and L. Yuan, "REVIVE: regional visual representation matters in knowledge-based visual question answering," in *Advances in Neural Information Processing Systems*, 2022.